SCIENCE CHINA
Earth Sciences

• RESEARCH PAPER •

May 2010 Vol.53 No.5: 721–730
doi: 10.1007/s11430-009-0203-z

Retrieving crop leaf area index by assimilation of MODIS data into a crop growth model

WANG DongWei[1,2,3], WANG JinDi[1,2*] & LIANG ShunLin[4]

[1] *State Key Laboratory of Remote Sensing Science, Jointly Sponsored by Beijing Normal University and Institute of Remote Sensing Applications, CAS, Beijing 100875, China;*
[2] *School of Geography, Beijing Key Laboratory of Environmental Remote Sensing and Digital City, Beijing Normal University, Beijing 100875, China;*
[3] *Haihe River Water Conservancy Commission, Tianjin 300170, China;*
[4] *Department of Geography, University of Maryland, College Park, MD 20742, USA*

Received June 30, 2009; accepted September 10, 2009; published online March 30, 2010

Leaf area index (LAI) is an important parameter in monitoring crop growth. One of the methods for retrieving LAI from remotely sensed observations is through inversion of canopy reflectance models. Many model inversion methods fail to account for variable LAI values at different crop growth stages. In this research, we use the crop growth model to describe the LAI changes with crop growth, and consider *a priori* LAI values at different crop growth stages as constraint information. The key approach of this research is to assimilate multiple canopy reflectance values observed at different growth stages and *a priori* LAI values into a coupled crop growth and radiative transfer model sequentially using a variational data assimilation algorithm. Adjoint method is used to minimize the cost function. Any other information source can be easily incorporated into the inversion cost function. The validation results show that the time series of MODIS canopy reflectance can greatly reduce the uncertainty of the inverted LAI values. Compared with MODIS LAI product at Changping and Shunyi Counties of Beijing, this method has significantly improved the estimated LAI temporal profile.

inversion, leaf area index, crop growth model, time series, MODIS

Citation: Wang D W, Wang J D, Liang S L. Retrieving crop leaf area index by assimilation of MODIS data into a crop growth model. Sci China Earth Sci, 2010, 53: 721−730, doi: 10.1007/s11430-009-0203-z

Leaf area index (LAI) is an important structural parameter of vegetation canopies, which is crucial for modeling canopy interception, evapotranspiration, and net photosynthesis. In recent years, there has been considerable interest in developing algorithms for retrieving LAI from remotely sensed observations [1–4]. Many efforts have been made to retrieve LAI through its statistical relationship with spectral vegetation indices (VI), physical model inversion or other nonparametric methods. Using VIs for LAI retrieval is simple; however, the inversion results always have large uncertainties. Canopy radiative transfer models physically describe the relationship between canopy structural and optical parameters and canopy reflectance. Model inversion is a reverse process, which starts from an inversion cost function. Efforts have been made to invert LAI using prior information of model parameters [5–7]. However, an obvious drawback is the difficulty in obtaining *a priori* information. Nonparametric methods (e.g., neural network [8–10]) provide another means for LAI retrieval by partly using physical or statistical information. Although some attempts have been made to use temporal signatures of remote sensing [11, 12], most studies have not estimated LAI using the temporal

*Corresponding author (email: wangjd@bnu.edu.cn)

profiles of observations.

For different applications, integrating multi-temporal remote sensing data with crop growth simulation models is recognized as a promising approach [13]. Several schemes of integrating a crop growth model with remote sensing data possessing various degrees of complexity have been developed in the last ten years, as reviewed by Fischer et al. [14], Moulin et al. [15] and Qin et al. [4]. Bach et al. [16] experimented with coupling a raster-based PROMET-V model with the radiative transfer model GeoSAIL to predict biomass and yield. Guérif et al. [17] and Launay et al. [18] combined the SUCROS crop model with the SAIL canopy reflectance model for accurate estimation of sugar beet yield. The SAIL model has also been integrated with the EPIC crop model to estimate the spring wheat yield in North Dakota [19]. Doraiswamy et al. [20] used a look-up table (LUT) method to estimate LAI from 250 m MODIS reflectance data. The crop- modeled LAI was adjusted to fit the MODIS simulated LAI by changing planting time, time of maximum LAI attainment, and the onset of leaf senescence. Koetz et al. [21] have also used LUT to produce simulated reflectance to construct the inversion cost function for LAI retrieval, and the semi-mechanistic model CSDM was used to smooth estimated LAI from multi-temporal remote sensing observations in two successive steps. Ma et al. [22] used the WOFOST crop growth model coupled to SAIL-PROSPECT for minimizing the differences between simulated and synthesized SAVI from remote sensing data to monitor winter wheat growth at the potential production level. Aiming to improve the accuracy of wheat yield predictions, Dente et al. [23] incorporated leaf area index retrieved from ENVISAT ASAR and MERIS data into the CERES-Wheat crop growth model. Results indicate that LAI maps retrieved from MERIS and ASAR data can be effectively assimilated into the CERES-Wheat model thus leading to accuracies of the yield maps ranging from 360 kg/ha to 420 kg/ha. A practical procedure using the variational optimization method to predict crop yield at the regional scale from MODIS data was recently developed by Fang et al. [24]. This method outputs agronomic variables (yield, planting, emergence and maturation dates) and biophysical parameters (e.g., LAI).

In this study, *a priori* information about the LAI temporal profile, which varies with different growth stages and which is described by crop growth model and LAI climatology, is used to retrieve LAI. A variational data assimilation strategy is developed to adjust crop growth model input parameters using remote sensing observations and prior LAI temporal profiles optimally. In this procedure, remote sensing canopy reflectances are assimilated by using a radiative transfer model to establish a relationship with LAI simulated by the crop growth model, and the prior LAI temporal profile is directly assimilated. The inverted LAI is estimated by minimizing the inversion cost function, which has included the crop growth model, remotely sensed reflectance, and prior LAI temporal profile. This method is tested using MODIS data over winter wheat at Changping and Shunyi counties of Beijing, China.

1 Methods

1.1 Crop growth model

The crop growth model CERES-Wheat is used in this study. CERES-Wheat is a dynamic model under the DSSAT shell that has different modules for different kinds of crops [25]. The CERES-Wheat model simulates growth, development, and yield of the cereal crop by taking into account the effects of genetics, weather, soil conditions, and crop management. This model offers the ability to evaluate options for increasing yield, water, and nitrogen use efficiencies. It enables us to input biological and physical parameters, and obtain user-specified objectives. In addition to LAI dynamics, the CERES-Wheat model also simulates the water and nitrogen balances of the soil-vegetation-atmosphere system using a daily step.

1.2 Prior LAI knowledge

We have incorporated *a priori* LAI values into the inversion cost function. To obtain this kind of prior information, we use the statistical results of LAI values at different growth stages from the Chinese spectrum library created in 2004 [7], which contain the representative spectra of typical land surface types in China. One of the goals in constructing this library is to provide prior knowledge for remote sensing model inversion. More than 20000 crop spectra are included, such as wheat, maize, and rice. Relevant crop structural parameters, component parameters, leaf and soil spectra were also collected. Some early data were measured more than 20 years ago [26]. Wang et al. [27] presented the statistical results of LAI concerned more than 1000 measurements on winter wheat from the Chinese spectrum library, and all LAI values of winter wheat in the same phenological stage were used for statistical analysis. The mean and variance of LAI values with phenological stages are shown in Figure 1, and used to obtain a fitting curve as prior LAI temporal profile in this study as below.

Uncertainty ranges of *a priori* LAI values of statistical results vary for different phenological stages. To match these statistical results at phenological stages with the corresponding observation time of remote sensing observation in the inversion cost function, we first transformed the phenological stage to the day of year (DOY) by using the observation date of this stage recorded in the spectrum library. Second, we obtained one fitting eq. (1a) to describe the prior mean of LAI, with DOY as the independent variable and the statistical mean of LAI as the dependent variable. Another fitting eq. (1b) describing prior LAI variance was also obtained by using the same method. Thus, we can

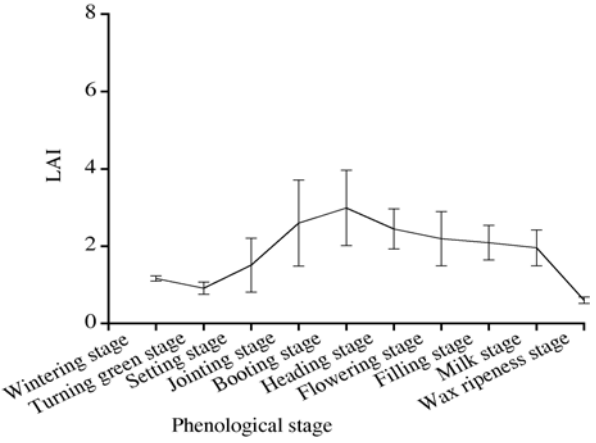

Figure 1 LAI statistical results of winter wheat.

obtain the prior LAI information when an arbitrary DOY is given:

$$LAI_J = p_0 + p_1 d + p_2 d^2 + p_3 d^3, \tag{1a}$$

$$LAI_Q = q_0 + q_1 d + q_2 d^2 + q_3 d^3, \tag{1b}$$

where LAI_J and LAI_Q are the fitted mean and variance of *LAI*, respectively; d is remotely sensed observation date, denoted as DOY; p_i and q_i are the coefficients. Eqs. (1a) and (1b) describe the LAI growth trend with DOY and its uncertainty, and can be used as prior ground LAI information. For application, the spatial resolution of prior LAI knowledge can be consider to match the remotely sensed observation because the sources of prior LAI data coming from an extensive region (more in North China), and be included in Chinese spectrum library.

1.3 Inversion cost function

To retrieve LAI from multiple information sources, we incorporated *a priori* LAI values, remotely sensed observations and a crop growth model into the inversion cost function. The parameters that are sensitive to LAI in the crop growth model are adjusted by minimizing the cost function. Remotely sensed observations are used sequentially; the posterior variance of the adjusted parameters are obtained and used to update the background of the adjusted parameters. The inversion cost function is denoted as follows:

$$J_B(\boldsymbol{x}_0) = \frac{1}{2}(\boldsymbol{x}_0 - \boldsymbol{x}_B)^{\mathrm{T}} \boldsymbol{B}^{-1}(\boldsymbol{x}_0 - \boldsymbol{x}_B), \tag{2a}$$

$$J_\tau^Q(\boldsymbol{x}_0) = \frac{1}{2}\int_0^\tau (LAI_t - LAI_t^B)^{\mathrm{T}} \boldsymbol{C}_t^{-1}(LAI_t - LAI_t^B)\mathrm{d}t, \cdot\frac{1}{2}\int_0^\tau (\boldsymbol{y}_t - H_t(\boldsymbol{x}_0))^{\mathrm{T}} \boldsymbol{Q}_t^{-1}(\boldsymbol{y}_t - H_t(\boldsymbol{x}_0))\mathrm{d}t, \tag{2b}$$

$$J_\tau(\boldsymbol{x}_0) = J_B(\boldsymbol{x}_0) + J_\tau^Q(\boldsymbol{x}_0) + \int_0^\tau \lambda(t) G_t(\boldsymbol{x}_0)\mathrm{d}t, \tag{2c}$$

where x_0 is the vector of the adjusted parameters which will be clear in latter section 3, and the initial inputs of the crop growth model $G_t(x_0)$; x_B is the prior value vector of the adjusted parameters, B is the prior value covariance matrix of x_B; LAI_t is the LAI value at time t, and LAI_t^B is the prior value of LAI_t fitted by using the method described in Section 2.2; C_t is the prior variance at time t which can also be obtained by fitting; y_t is remotely sensed reflectance at time t, and $H_t(x_0)$ is the mapping operator which is the coupled canopy growth and radiative transfer model for calculating the crop reflectance based on the adjusted parameters, Q_t denotes the covariance matrix of remotely sensed observations and mapping operator $H_t(x_0)$; Integral symbol indicate that all of useful information from time t=0 to τ will be included in cost function. In eq. (2c), $\lambda(t)$ is used as a Lagrangian multiplier, and $G_t(x_0)$ describes the evolution process of the state variable LAI_t. Eq. (2c) is general method for multi-sources data assimilation, and it can be found in Kalnay's classical book [28].

Prior knowledge of the adjusted parameters is incorporated into the inversion cost function through eq. (2a), and prior knowledge of LAI is incorporated by the first term of eq. (2b). The second term of eq. (2b) is the forcing term of remotely sensed observations. We combine eqs. (2a), (2b) and the state eq. $G_t(x_0)$ into eq. (2c) by using a Lagrangian multiplier. Because this is a strong constraint problem, inverted LAI values will be retrieved from the crop growth model using optimal adjusted parameters. So our goal of constructing the inversion cost function (2c) can be considered as finding an optimal temporal profile of LAI in the profiles set coming from the state eq. $G_t(x_0)$. The retrieved LAI temporal profile is resulted from *a priori* adjusted parameters, *a priori* LAI values, and the time series of remotely sensed observations.

The optimal adjusted parameters are determined from the inversion cost function (2c) through a step-by-step variational optimization procedure. The posterior mean and variance of the adjusted parameters from the previous inversion step are used in the current step. In this paper, the canopy radiative transfer model SAIL [29] that is coupled with the CERES-Wheat model is used as the mapping operator H; MODIS surface reflectance products (MOD09) are used as y_t; and the crop growth model CERES-Wheat is used as $G_t(x_0)$. Here LAI_t is the output of the crop growth model at time t.

Minimizing the inversion cost function (2c) is a complicated problem because of the complexity of the coupled crop radiative transfer and growth model. In this study, we handle the crop growth model as follows:

Considering LAI as a dependent variable, we can denote crop growth model as eq. (3):

$$\frac{\partial LAI_t}{\partial t} = K(LAI_t), \qquad 0 \leqslant t \leqslant \tau, \qquad LAI(0) = LAI_0 = V(x_0), \tag{3}$$

where K denotes the differential operator of the crop growth model, and LAI_0 is the initial LAI value. This is a differential equation with LAI_0 as boundary condition at t=0. In fact, we can not determine LAI_0 definitely, but LAI_0 can be produced according to the adjusted parameters by letting $LAI(0)=LAI_0=V(x_0)$ so that the differential equation's boundary condition is denoted as the adjusted parameters implicitly.

According to eq. (3), we rewrite eq. (2c) as a strong constraint problem as follows,

$$J_\tau(x_0) = J_B + J_\tau^Q + \int_0^\tau \lambda(t)\left(\frac{\partial LAI_t}{\partial t} - K(LAI_t)\right)\mathrm{d}t, \quad (4a)$$

$$0 \leqslant t \leqslant \tau,$$

$$LAI(0) = LAI_0 = V(x_0), \quad (4b)$$

where eq. (4b) is the initial boundary condition of the crop growth model. Thus, every term in cost function (4a) can be expressed as a function of the adjusted parameters x_0. Since it has been extensively used in other scientific disciplines and our previous study [4], the adjoint method can be used to minimize the cost function.

Above cost function can be solved to obtain the analytical solution of the variational assimilation algorithm by solving the Eular-lagrange equation iteratively. In practical application, the optimization method will be used to realize this algorithm [30]. In this paper, a conjugated gradient method is used to minimizing the inversion cost function, and the necessary gradient is obtained using adjoint method described as mentioned above. The new optimization was performed when an available observation was incorporated into inversion cost function. Every optimization process stops when the inversion cost function varies less than 1% between two consecutive iterations.

1.4 Canopy radiative transfer model SAIL

In this paper, we will use $\partial H_t^T / \partial LAI_t$ in optimization which is the gradient of LAI from the radiative transfer model SAIL. It related the radiative transfer model SAIL to adjusted parameters. However, the parameter LAI is hidden in the coefficients of SAIL. To get $\partial H_t^T / \partial LAI_t$, we use the tangent linear equations of the SAIL model around LAI. These equations can be denoted as follows:

$$\frac{\mathrm{d}\hat{E}_s}{\mathrm{d}x} - K\hat{E}_s - \hat{K}E_s = 0, \quad (5a)$$

$$\frac{\mathrm{d}\hat{E}^-}{\mathrm{d}x} + S\hat{E}_s + \hat{S}E_s - a\hat{E}^- - \hat{a}E^- + \sigma\hat{E}^- + \hat{\sigma}E^+ = 0, \quad (5b)$$

$$\frac{\mathrm{d}\hat{E}^+}{\mathrm{d}x} - S'\hat{E}_s - \hat{S}'E_s - \sigma\hat{E}^- - \hat{\sigma}E^- + a\hat{E}^+ + \hat{a}E^+ = 0, \quad (5c)$$

$$\frac{\mathrm{d}\hat{E}_0}{\mathrm{d}x} - w\hat{E}_s - \hat{w}E_s - v\hat{E}^- - \hat{v}E^- - u\hat{E}^+ - \hat{u}E^+ + k\hat{E}_0 + \hat{k}E_0 = 0, \quad (5d)$$

where $\hat{E}_s$, $\hat{E}^-$, $\hat{E}^+$, $\hat{E}_0$ are differentials of radiance with regard to LAI. $\hat{K}$, $\hat{S}$, $\hat{S}'$, $\hat{a}$, $\hat{\sigma}$, $\hat{u}$, $\hat{v}$, $\hat{w}$, $\hat{k}$ are differentials of SAIL model coefficients triggered by the differential of LAI. Eqs. (5a)–(5d) represent the radiance differentials due to the LAI differential, so that the SAIL model gradient around LAI can be obtained from the limit of the ratio of observation radiance differential to LAI differential.

1.5 Updating the prior knowledge of the adjusted parameters

So far, we have used all remotely sensed observations before time τ. The prior knowledge of the adjusted parameters can be updated as follows. As a new remotely sensed observation is available at τ+1, the inversion cost function becomes

$$\begin{aligned} J_{\tau+1}(x_0) = {} & J_\tau^B(x_0) + J_\tau^Q(x_0) + \\ & (LAI_{\tau+1} - LAI_{\tau+1}^B)^{\mathrm{T}} C_{\tau+1}^{-1}(LAI_{\tau+1} - LAI_{\tau+1}^B) + \\ & (y_{\tau+1} - H_{\tau+1}(x_0))^{\mathrm{T}} Q_{\tau+1}^{-1}(y_{\tau+1} - H_{\tau+1}(x_0)) \\ & + \int_0^{\tau+1} \lambda(t) G_t(x_0)\mathrm{d}t, \end{aligned} \quad (6)$$

where $J_\tau^B(x_0)$ is obtained from the previous inversion step. The posterior covariance can be calculated according to Yang et al. [31]:

$$B_{\tau+1} = \left(\sum_{t=1}^{\tau}(LAI_t'^{\mathrm{T}} C_t^{-1} LAI_t' + H_t'^{\mathrm{T}} Q_t^{-1} H_t') + B_\tau^{-1}\right)^{-1}, \quad (7)$$

where LAI_t' is the Jacobi matrix of LAI_t about xo; H_t' is the Jacobi matrix of the SAIL model about LAI_t; In eq. (7), the term in outer parentheses is the Hessian matrix of the first term and the second term in cost function (2b). Eq. (7) describes the posterior variance of the adjusted parameter obtained from the least squares rule.

Inversion cost function (4a) combines three types of useful information: remotely sensed observations, coupled crop radiative transfer and growth model and *a priori* LAI values. The prior knowledge of the adjusted parameters is updated by eq. (7). In this process, the cost function is first calculated using the first remotely sensed observation and *a priori* LAI information. After obtaining the solutions of the adjusted parameters, the cost function is updated by combining next remotely sensed observation and *a priori* LAI information accordingly, and the prior knowledge term of the adjusted parameters of eq. (4a) is substituted by the posterior information obtained from the previous iteration step. The whole process iterates until the final remote sensing observation has been used. Note that the solutions of the adjusted parameters are inputted to the crop growth model in each step to simulate LAI as our estimate. The optimal LAI values are obtained from the last inversion step.

2 Results analysis

To test the methodology described above, we inverted the winter wheat LAI from MODIS observations at Changping and Shunyi counties, Beijing. The geographic area is represented by the following latitude and longitude readings in the WGS84 coordinate system: (40.3383°N, 116.4111°E) (upper left); (39.9686°N, 116. 8008°E) (lower right). The location of this geographic area is shown in Figure 2.

We carried out an experiment to investigate winter wheat's growth status under different management conditions in 2004. The total experiment area is about 167 hectares. Twenty-two sub-grids were designed for different crop management conditions. The central coordinates are 40.1831°N, 116.4385°E. In this experiment, some growth parameters about winter wheat were measured and recorded, such as planting density, row space, phenological stage, leaf water content, leaf angle distribution and so on. LAI was also measured periodically. We used these measured LAI values to validate our algorithm. The LAI mean of all sub-grids is calculated as the true LAI value because every sub-grid is too small to represent the LAI value of one MODIS pixel. We also calculated the standard deviation of these measured LAIs in the 22 sub-grids to describe the uncertainty of the calculated true LAI values. The corresponding MODIS pixel of 22 sub-grids is located in the upper left corner of the processed MODIS image, and marked as Point1.

In the LAI retrieval procedure, the adjusted parameters include thermal time per leaf (PHINT), relative vernalization sensitivity of seed (P1V), initial soil water content (SW), initial soil NO_3 content (NO_3), initial soil NH_4 content (NH_4), fertilizer amount (ANFER), and irrigation amount (AMIR). These parameters were selected due to their sensitivity to LAI. For field experiments in 2004, we simulated the LAI by this crop growth model and found that LAI varied largely with PHINT. LAI has varied 50% in extreme situations when using PHINT=90 as reference. For initial NH_4, NO_3 and SW parameters, large sensitivities to LAI were shown when water and nutrition are not enough. Similarly, irrigation and fertilizer amounts showed large sensitivity to LAI when initial NH_4, NO_3 and SW are not enough. We also found that irrigation, fertilizer and NH_4, NO_3, SW are affected mutually. In some extreme situations, LAI has 4 variations. Although other parameters (e.g., field moisture capacity and planting date) also show some sensitivity to LAI, we did not consider them useful for applications. For future applications, we will establish a database to provide some general parameters such as planting date, and invariable soil parameters in this area. In the current study, selecting the adjusted parameters is based on their sensitivities to LAI, and variations over our study area.

Figure 2 Geographic location of research area in Beijing, China.

The MODIS land surface reflectance product (MOD09) is used as remotely sensed observations with three bands: 1 (620–670 nm), 2 (841–876 nm) and 5 (1230–1250 nm). It covers DOYs 105, 113, 121, 129, 137, 145, 153, 161, long enough for winter wheat growth. MOD09 is an 8-day composite of MODIS 500 m Level 2G products. For example, MOD09 DOY 105 involved data from DOY 105 to DOY 112. Every corresponding pixel value in this MOD09 product is the observation value, which has the best Quality Control (QC) value within 8 days. Therefore, the true observation date for every MOD09 pixel is different from the nominal MOD09 product date. Fortunately, these true observation dates are recorded in MOD09 product. For our eight MOD09 datasets, these true DOYs are 107, 118, 125, 134, 139, 152, 154, and 162.

In this paper, the initial values of the adjusted parameters are defined in such a way. The PHINT and P1V initial values are set to 90 and 2.5 based on the user guide of the CERES-Wheat model for general applications. Considering that the adjusted soil parameters are for 4 soil layers in depths 20, 55, 110, 150 centimeters and these are consistent with field investigation, the same initial values are set for all layers. The background SW is assumed to be 0.25 cm^3/cm^3. The background NO_3 and NH_4 are assumed to be 5.4 and 2.7 μg/g. The parameter ANFER is assumed to be 80 kg/ha. Finally, the AMIR is assumed as 60 mm, the irrigation and fertilizer management data are specified based on advice from the local agricultural research institute. The PHINT, P1V, NO_3, NH_4's uncertain ranges are assumed to be 30% of the background values. The AMIR's and ANFER's uncertain range are assumed to be 50% of the background value.

To examine the details, we selected four pixels from the image. One pixel is the experiment area pixel while the other three pixels were arbitrarily chosen. These pixels are

denoted as Point1, Point2, Point3 and Point4. These four points are marked on Figure 4(a). Point1 is the experiment area pixel.

2.1 Using prior LAI knowledge

Our method uses every MODIS observation in the temporal window and *a priori* LAI information to adjust the LAI profile based on cost function (2) and updating eq. (7).

Figure 3 compares the inverted LAI profiles with and without using *a priori* LAI information at Point1. Measured ground LAI and MODIS LAI are also plotted for comparison. Figure 3(a) is the inverted LAI value on DOY 107 using only the remotely sensed observation of DOY 107. We can find out that the inverted LAI value without using *a priori* LAI is higher than MODIS LAI, and inverted LAI using *a priori* LAI information which in the uncertain range of measured LAI is higher than that without using *a priori* LAI information. Figure 3(b) to (h) compares the inverted LAI profiles using MODIS observations of DOYs 118, 125, 134, 139, 152, 154, and 162. By comparing these inverted LAI values with the measured LAI values, we find that the inverted LAI values using *a priori* LAI information are more reasonable than the inverted LAI values obtained without using *a priori* LAI values and MODIS LAI values. The aim of incorporating *a priori* LAI information into the

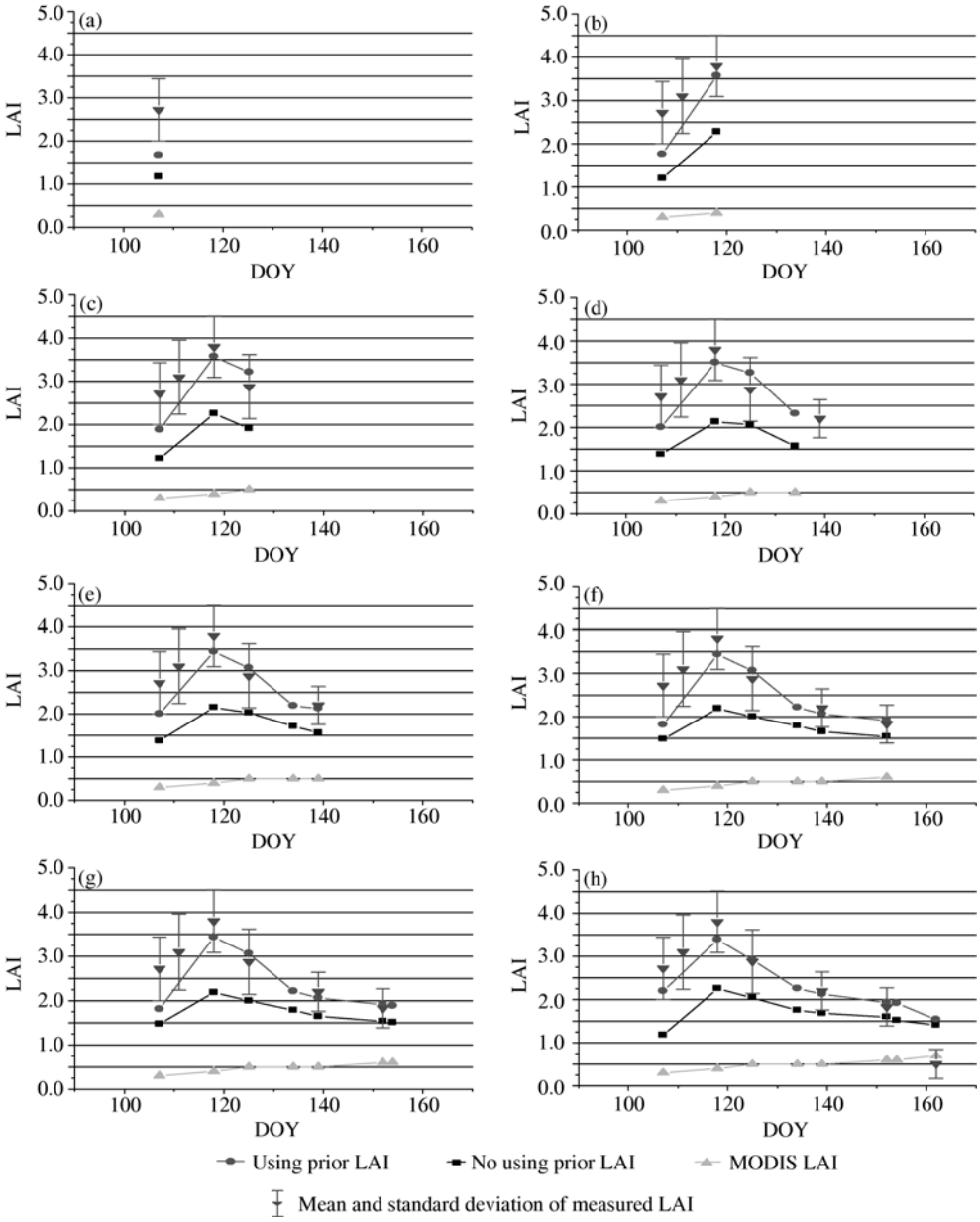

Figure 3 LAI inversion with and without *prior* LAI information. (a) Only using one observation; (b) introducing two observations; (c) introducing three observations; (d) introducing four observations; (e) introducing five observations; (f) introducing six observations; (g) introducing seven observations; (h) introducing eight observations.

inversion cost function is to improve the LAI estimation when remotely sensed observations could not provide enough in- formation for the successful LAI inversion, which has been demonstrated in Figure 3(a)–(h).

Because of the constraint of the crop growth model, the LAI values retrieved even without using *a priori* LAI information are also more reasonable than MODIS LAI values, although they are much lower than the measured LAI values.

2.2 The inverted and MODIS LAI values

Because crop growth model and *a priori* LAI information are included in the inversion cost function, the inverted LAI values follow the phenology of the normal crop growth. The inverted LAI and MODIS LAI images are shown in Figures 4 and 5. In Figure 4, the corresponding DOY of the reflectance observation is listed in parentheses; these DOYs are also the DOYs of our inverted LAI. In Figure 5, MOD15 LAI products use all available observed reflectance in an 8-day range to invert LAI, so for MOD15 LAI products of DOY 105, we thought it is representing the LAI values of DOY 109; other MOD15 LAI products of different DOY are thought similarly, and they are listed in parentheses. It is evident that our results in Figure 4 better characterize the normal growth status, with an ascending trend from DOY 105(107) to DOY 113(118). In fact, the winter wheat of this area grows very fast during this period. After DOY 113(118), a decreasing trend can be found in Figure 4, matching the phenology of the growth status of winter wheat in this area. But in Figure 5, the MODIS LAI product shows a flat LAI profile from DOY 105(109) to DOY 161(165).

The LAI profiles of the inverted LAI values and MODIS LAI product for these four pixels are plotted in Figures 6 and 7, respectively. We find that four MODIS LAI profiles do not change much from DOY 105(109) to DOY 161(165). There are some "valleys", which does not make sense from the crop growth rule. Another problem is that MODIS LAI values of all four pixels are lower than 1.0, but we know clearly from field investigations that in these growth stages the winter wheat LAI of this area are higher than 1.0. In contrary to Figure 7, our inverted LAI values in Figure 6 have the normal range and a reasonable trend.

2.3 Updating background information of the adjusted parameters

The *a priori* knowledge of the adjusted parameters in inversion cost function (2) needs to be updated when every re-

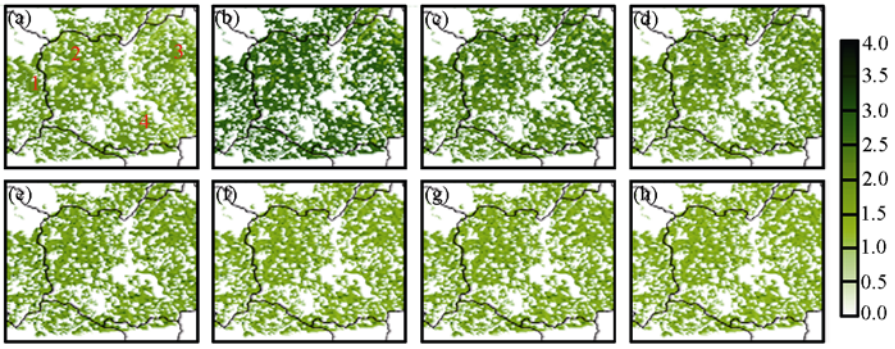

Figure 4 Inverted LAI maps. (a) DOY 105(107); 1, Point1; 2, Point2; 3, Point3; 4, Point4. (b) DOY 113(118). (c) DOY 121(125). (d) DOY 129(134). (e) DOY 137(139). (f) DOY 145(152). (g) DOY 153(154). (h) DOY 161(162).

Figure 5 MODIS LAI maps. (a) DOY 105(109); (b) DOY 113(117); (c) DOY 121(125); (d) DOY 129(133); (e) DOY 137(141); (f) DOY 145(149); (g) DOY 153(157); (h) DOY 161(165).

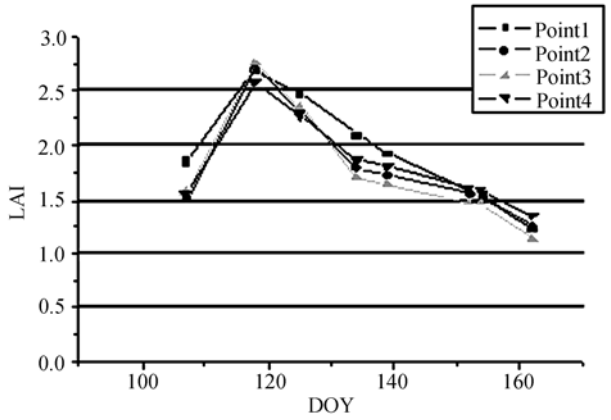

Figure 6 Inverted LAI using our method.

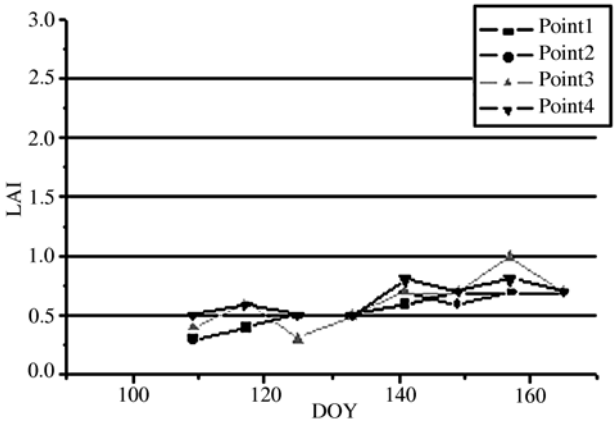

Figure 7 MODIS LAI product.

motely sensed observation is incorporated into eq. (2). The updated information is the prior mean and covariance of the probability distribution of the adjusted parameter, which are x_B and B terms in eq. (2) respectively. Because prior knowledge of the adjusted parameters is poorly known in reality, we set a high initial uncertainty for the adjusted pa-meters. For example, PHINT describes thermal time value when a new leaf grows (CERES-Wheat assumes that only one new leaf grows every time). We do not have *a priori* knowledge of PHINT, so we adopt the suggested value in CERES-Wheat's user guide for this parameter as the *a priori* expectance, and a potential uncertainty range as *a priori* standard deviation. We updated this *a priori* knowledge when a new remotely sensed observation is incorporated into the cost function according to eq. (7), which lowers the uncertainty of this parameter. Figure 8 shows the updating of *a priori* knowledge by using PHINT as an example. The uncertainty range is lowered when every MODIS observation is incorporated.

Table 1 lists the means of the updated variances of all four points sequentially. This shows the updating trend of our inversion method and implies that every MODIS ob-

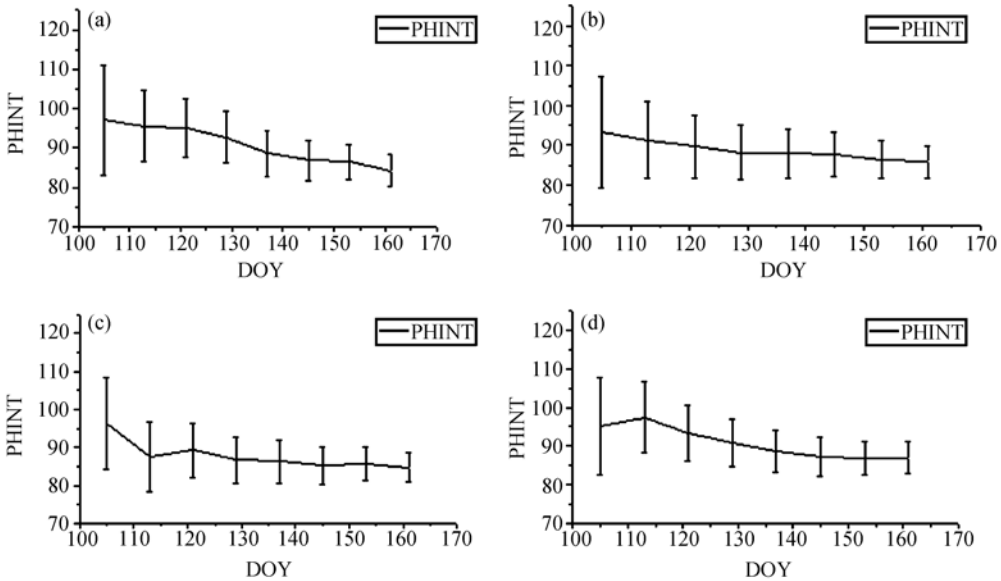

Figure 8 PHINT error updating of Point1–Point4. (a) Error updating of Point1; (b) error updating of Point2; (c) error updating of Point3; (d) error updating of Point4.

Table 1 Mean variance trend of PHINT of four points

Time step	1	2	3	4	5	6	7	8
PHINT error	349.3	172.5	112.2	87.1	71.0	51.2	42.7	23.6

servation of the time series provides extra information for the adjusted parameters. Accumulation of this kind of information definitely reduces parameters' uncertainty.

3 Discussion and conclusions

Traditional LAI inversion methods in remote sensing consider only the information of remotely sensed observation at individual times. The relationship of LAIs at different growth stages has not been effectively used in the inversion process. In this paper, we combine the time series of remotely sensed observations and the crop growth model into the inversion cost function that is minimized by a variational data assimilation method. The inverted LAI depends not only on remotely sensed observations but also on the crop growth model. Time series of remotely sensed observations are used to adjust the parameters of the crop growth model, and the crop growth model provides extra information for the inverted LAI. This method ensures that the inverted LAI values at different crop growth stages satisfy the crop growth rule. Because of the regional differences of winter wheat growth, we have also incorporated *a priori* LAI information into the inversion cost function. Thus, the inversion cost function is constrained by remotely sensed observations, crop growth model, and *a priori* LAI knowledge.

Our validation results demonstrate that the inverted LAIs are effectively improved by incorporating the extra prior knowledge of LAI. These results can better characterize the LAI's true values than just incorporating the crop growth model in the inversion function.

One issue in this approach is the difference between the MODIS observation scale and the scale of the measured LAI. This scale mismatch partially accounts for the difference between inverted LAIs and the measured LAIs. The spatial resolution of MOD09 data is 500 m and many pixels are mixed in our research area. Pixel mixture is a potential factor affecting the inversion accuracy. By using the land use type map from TM image, we found that our twenty-two sub-grids cover about 80% of the MODIS pixel, with other land use types including road and water also within this pixel. If the inverted LAIs are divided by 0.8, they match with the ground measurements much better (Figure 3).

We used only temporal information of remotely sensed observations in this study; however, the contextual information among the neighboring pixels is also valuable. This could potentially improve the accuracy of the inverted LAI by integrating multiple data sources.

The authors thank the all participants of the 863 Project-Chinese spectrum library for their excellent works on winter wheat canopy reflectance and LAI measurements, and we thank Dr. Carol Russell for her help in improving the presentation of this manuscript. This work was supported by the National Natural Science Foundation of China (Grant Nos. 40871163, 40571107), the Beijing Natural Science Foundation (Grant No. 4083035), the National Basic Research Program of China (Grant No. 2007CB714407), the Program for Key International Science and Technique Cooperation Project of China (Grant No. 2004DFA06300).

1 Baret F, Buis S. Estimating canopy characteristics from remote sensing observations: Review of methods and associated problems. In: Liang S, ed. Advances in Land Remote Sensing: System, Modeling, Inversion and Application. Springer Science+Business Media BV, 2008. 173–202
2 Liang S. Quantitative Remote Sensing of Land Surfaces. New York: John Wiley and Sons Inc., 2004
3 Liang S. Recent developments in estimating land surface biogeophysical variables from optical remote sensing. Prog Phys Geogr, 2007, 31: 459–470
4 Qin J, Liang S, Li X, et al. Development of the adjoint model of a canopy radiative transfer model for sensitivity study and inversion of leaf area index. IEEE Trans Geosci Remote Sens, 2008, 46: 2028–2037
5 Li X, Wang J, Hu B, et al. On utilization of *a prior* knowledge of remote sensing models. Sci China Ser D-Earth Sci, 1998, 41: 580–586
6 Qu Y, Wang J, Wan H, et al. A Bayesian network algorithm for retrieving the characterization of land surface vegetation. Remote Sens Environ, 2008, 112: 613–622
7 Wang J, Li X. Knowledge database and inversion. In: Liang S, ed. Advances in Land Remote Sensing: System, Modelling, Inversion and Application. Springer Science+Business Media BV, 2008. 203–218
8 Fang H, Liang S. Retrieving leaf area index with a neural network method: Simulation and validation. IEEE Trans Geosci Remote Sens, 2003, 41: 2052–2062
9 Fang H, Liang S. A hybrid inversion method for mapping leaf area index from MODIS data: Experiments and application to broadleaf and needleleaf canopies. Remote Sens Environ, 2005, 94: 405–424
10 Smith J A. LAI inversion using a back-propagation neural network trained with a multiple scattering model. IEEE Trans Geosci Remote Sens, 1993, 31: 1102–1106
11 Liang S, Schaepman M, Kneubuhler M. Remote sensing signatures: Measurements, modeling and applications. In: Li Z, Chen J, Baltsavias M, eds. Advances in Photogrammetry, Remote Sensing and Spatial Information Science, ISPRS Congress Book. Balkema: CRC Press, 2008. 127–143
12 Xiao Z, Liang S, Wang J, et al. A temporally integrated inversion method for estimating leaf area index from MODIS data. IEEE Trans Geosci Remote Sens, 2009, 47: 2536–2545
13 Liang S, Qin J. Data assimilation methods for land surface variable estimation. In: Liang S, ed. Advances in Land Remote Sensing: System, Modeling, Inversion and Applications. Springer Science Business Media BV, 2008. 319–339
14 Fischer A, Kergoat L, Dedieu G. Coupling satellite data with vegetation functional models: Review of different approaches and perspectives suggested by the assimilation strategy. Remote Sens Rev, 1997, 15: 283–303
15 Moulin S, Bondeau A, Delecolle R. Combining agricultural crop models and satellite observations: From field to regional scales. Int J Remote Sens, 1998, 19: 1021–1036
16 Bach H, Mauser W, Schneider K. The use of radiative transfer models for remote sensing data assimilation in crop growth models. In: Stafford J, Werner A, eds. Precision Agriculture: Papers from the 4th European Conference on Precision Agriculture. Berlin, Germany, 2003
17 Guérif M, Duke C L. Adjustment procedures of a crop model to the site specific characteristics of soil and crop using remote sensing data assimilation. Agric Ecosyst Environ, 2000, 81: 57–69
18 Launay M, Guerif M. Assimilating remote sensing data into a crop

model to improve predictive performance for spatial applications. Agric Ecosyst Environ, 2005, 111: 321–339
19 Doraiswamy P C, Moulin S, Cook P W, et al. Crop yield assessment from remote sensing. Photogramm Eng Remote Sens, 2003, 69: 665–674
20 Doraiswamy P C, Hatfield J L, Jackson T J, et al. Crop condition and yield simulation using Landsat and MODIS. Remote Sens Environ, 2004, 92: 548–559
21 Koetz B, Baret F, Poilve H, et al. Use of coupled canopy structure dynamic and radiative transfer models to estimate biophysical canopy characteristics. Remote Sens Environ, 2005, 95: 115–124
22 Ma Y, Wang S, Zhang L, et al. Monitoring winter wheat growth in North China by combining a crop model and remote sensing data. Int J Appl Earth Observ Geoinform, 2008, 10: 426–437
23 Dente L, Satalino G, Mattia F, et al. Assimilation of leaf area index derived from ASAR and MERIS data into CERES-Wheat model to map wheat yield. Remote Sens Environ, 2008, 112: 1395–1407
24 Fang H, Liang S, Hoogenboom G, et al. Crop yield estimation through assimilation of remotely sensed data into DSSAT-CERES. Int J Remote Sens, 2008, 29: 3011–3032
25 Hoogenboom G, Jones J W, Porter C H, et al. Decision Support System for Agrotechnology Transfer Version 4.0. Volume 1: Overview. Honolulu: University of Hawaii, 2003
26 Wang J, Li X. The spectrum knowledge base of typical object and remote sensing inversion of land surface parameters (in Chinese). J Remote Sensing, 2004, 8(Suppl): 4–7
27 Wang J, Zhang G, Xiao Y, et al. The prior knowledge of crop growth parameters constructed from the spectrum database of land surface objects (in Chinese). J Beijing Normal Univ (Nat Sci), 2007, 43: 284–291
28 Kalnay E. Atmospheric Modeling, Data Assimilation and Predictability. London: Cambridge University Press, 2002
29 Verhoef W. Light scattering by leaf layers with application to canopy reflectance modeling: The SAIL model. Remote Sens Environ, 1984, 16: 125–141
30 Wang X. Toward the objective analysis, four-dimensional assimialtion and adjoint methods (in Chinese). J PLA Univ Sci Technol, 2000, 1: 67–74
31 Yang X, Mu X, Wang D, et al. Retrieval of LAI by assimilating remotely sensed data into a simple crop growth model. In: Li M C, Ju W M, eds. Proceedings of Geoinformatics 2007. Nanjing: Nanjing University Press, 2007. 154–161